Modern Physics Letters B
1950088 (14 pages)

DOI: 10.1142/S021798491950088X

World Scientific
www.worldscientific.com

Enhanced electrical performance by modulation-doping in AlGaN-based deep ultraviolet light-emitting diodes

Sipan Yang*,†,‡,§, Miao He†,¶, Jianchang Yan‡,‖, Kunhua Wen†,
Junxi Wang‡, Yanan Guo‡ and Deping Xiong†

**School of Electronic Information and Electrical Engineering, Shanghai Jiao Tong University, Shanghai 200240, China*
†*School of Physics and Optoelectronic Engineering, Guangdong University of Technology, Guangzhou 510006, China*
‡*Research and Development Center for Solid State Lighting, Institute of Semiconductors, Chinese Academy of Sciences, Beijing 100083, China*
§*sheepoonyoung@sjtu.edu.cn*
¶*herofate@126.com*
‖*yanjc@semi.ac.cn*

Received 29 October 2018
Revised 21 December 2018
Accepted 2 January 2019
Published 11 March 2019

Through the silicon modulation-doping (MD) growth method, the electrical performance of AlGaN-based deep ultraviolet light-emitting diodes (DUV-LEDs) is improved by replacing the commonly uniform-doped (UD) method of n-AlGaN layer. The electroluminescence characterisic measurements demonstrate the MD growth method could effectively enhance the light emission intensity. Both the forward voltage and reverse leakage current of the MD samples are obviously reduced compared to those of the UD sample. Due to the existence of periodic Si-MD superlattices in n-AlGaN layers, which may behave like a series of capacitors, the built-in electric fields are formed. Both the measured capacitance–voltage (C–V) characteristics, and related photoluminescence (PL) intensity with the Si-MD growth method are enhanced. In detail, the effects of these capacitors can enhance the peak internal capacitance up to 370 pF in the MD sample, whereas the UD sample is only 180 pF. The results also mean that with better current spreading ability in the MD sample, the MD processes can effectively enhance the efficiency and reliability of DUV-LEDs. Thus, the investigations of the Si-MD growth methods may be useful for improving the electrical performance of DUV-LEDs in future works. Meanwhile, this investigation may partly suggest the minor crystalline quality improvements in the epi-layers succeeding the MD n-AlGaN layer.

Keywords: Ultraviolet light-emitting diodes; bias voltage; capacitance; n-AlGaN layer.

¶,‖Corresponding authors.

1. Introduction

AlGaN-based deep ultraviolet light-emitting diodes (DUV-LEDs) have been attracting considerable attention owing to their diverse applications, such as disinfection, sensing, water purification, bio-medical, general lighting and so on.[1–3] The internal capacitance measurements provide a useful method for a non-destructive testing of P–N junction and evaluation of the electrical parameters in DUV-LEDs.[4–6] For example, the capacitance–voltage (C–V) measurements are carried out simultaneously, which are frequently used to characterize the potential voltage characteristics due to the built-in electric fields (V_{bi}), the change of the depletion layer width (W_d), the dependence of the carrier concentration on the width of depletion regions, and the devices' stability for resisting the electro-static discharge (ESD) at different bias voltages.

To investigate the modulation-doping (MD) growth method, several research investigations such as p-type modulation-doped InGaN/GaN dot-in-a-wire for the most efficient phosphor-free white LEDs,[7] have been successfully performed. To further investigate the electrical performance in LEDs in detail, several approaches, like the research of C–V characteristics for devices' reliability,[8–10] have been widely studied. Also, other methods have been proposed to study the internal capacitance characteristics, such as the Si-delta doped techniques,[11–13] the Si-modulation-doped superlattice structure,[14] the methods with inserting three pairs of u-GaN/n-GaN layers between n-spacer layer and the active regions,[15] the growth process of modulation-doped GaN nanorods for the wide-band gap near UV-LEDs.[16] However, we also discovered some issues in the current research, in detail, most of these methods listed above were just to investigate the dependent properties of visible light LEDs or the nitride device systems, the modulation doping approach is new, and the influence of MD growth layer on AlGaN-based DUV-LEDs is rarely reported. Moreover, the validity of measured internal C–V characteristics for the electrical performance in DUV-LEDs has not been further published in the literatures.

In this study, we mainly focus on the different growth schemes of AlGaN:Si n-type layer first, and we further investigate two kinds of Si-doped growth methods of n-AlGaN layer in the context of DUV-LEDs, which are denoted as the Si-uniform doping (UD) samples and the MD samples, respectively. For the electrical characterization in these two prepared DUV-LED samples containing different kinds of AlGaN:Si n-side, the measurements of electroluminescence (EL) spectral emissions, current–voltage (I–V) characteristics, C–V characterizations and the related photoluminescence (PL) spectra are carried out, respectively. Moreover, the interrelationships within the electrical and optical performance, the device reliability, the internal capacitance are widely investigated.

2. Experimental Details

The studied AlGaN-based DUV-LEDs are grown by home-made metal organic chemical vapor deposition (MOCVD) system, Trimethylgallium (TMGa), trimethylaluminum (TMAI) and ammonia (NH_3) are used as Ga, Al and N sources, respectively. Silane and biscyclo-pentadienyl magnesium (Mg) are used as n-type and p-type dopants, respectively. Prior to the growth processes, the 430 μm thick sapphire substrates are treated in H_2 ambient. AlGaN-based DUV-LED structures are further grown on the 1 μm thick AlN template, which is commonly used as the buffer layers. The AlN/AlGaN superlattices (SLs) are grown first on the AlN buffer layer, which is composed of 20 cycles of a 20 nm thick AlN layer and 30 nm thick $Al_{0.4}Ga_{0.6}N$ layer. The following layers include a 2 μm thick high Al content n-$Al_{0.6}Ga_{0.4}N$ epi-layer, and there are two different kinds of Si-doped growth methods of n-AlGaN layer in every DUV-LED samples. For simplicity, the cross-sectional schematic structures of these two AlGaN-based wafer samples are exhibited below, as shown in Figs. 1(a) and 1(b).

In detail, sample A is labeled with the characteristics of Si-UD n-$Al_{0.6}Ga_{0.4}N$ layer, which is regarded as the reference sample for comparative study, and the SiH_4 flow rate is always set for 50 sccm. Sample B is labeled with the characteristics of Si-MD n-$Al_{0.6}Ga_{0.4}N$ layer with 40 periods SLs, and each period includes 2 layers of n-$Al_{0.6}Ga_{0.4}N$ grown in the mode of 30 sccm and 70 sccm SiH_4 flow rate, respectively. The growth temperature of the n-$Al_{0.6}Ga_{0.4}N$ layer of these two samples is about 1080°C. The schematic of these two Si-doping growth processes of the n-AlGaN layer is plotted below, as shown in Figs. 2(a) and 2(b). The multiple quantum wells (MQWs) is correspondingly grown on the n-AlGaN layer, which consists of additional 5 cycles of 12 nm thick $Al_{0.5}Ga_{0.5}N$ barriers and 2.4 nm thick $Al_{0.4}Ga_{0.6}N$ wells. After the MQWs, there is a 30 nm thick Mg-doped p-$Al_{0.6}Ga_{0.4}N$ electron-blocking layer (EBL), and the 160 nm thick p-GaN layer is grown thereon.

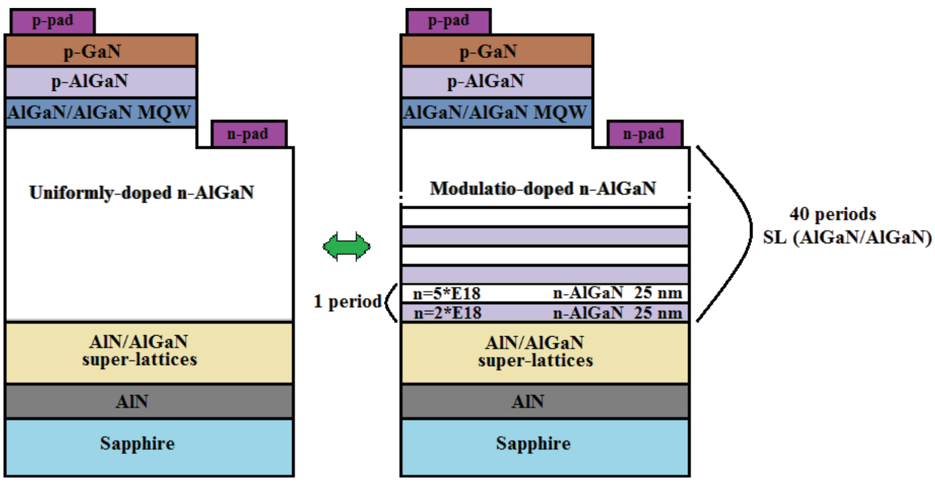

Fig. 1. The schematic structures of these two fabricated DUV-LED samples. (a) Sample A is with the characteristics of Si-UD growth method in n-AlGaN layer, which is denoted as the reference sample and (b) sample B is with the characteristics of Si-MD growth methods. The main difference between these two samples is marked with a bidirectional arrow.

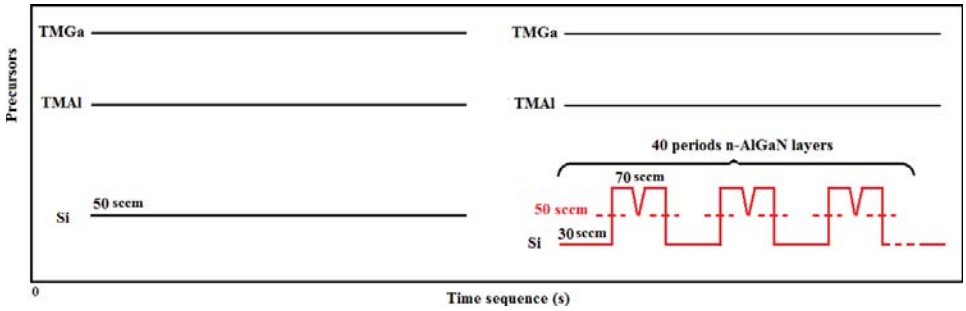

Fig. 2. The schematic graphs of the growth processes for these two samples. (a) Si-UD growth methods of n-AlGaN layer and (b) MD growth methods.

After the epitaxial growth, in order to activate the Mg acceptors under the appropriate annealing conditions, p-type layers in these two samples were annealed at 800°C within the reactor in flowing nitrogen (N_2) mode for 20 min. Both of these two devices are fabricated with a die size of 560 μm $*$ 560 μm by conventional DUV-LED structure methods, and the standard device processing of mesa etching down to n-AlGaN layer are employed in our experiments. A Ti/Al/Ti/Au metal stack is deposited on the n-AlGaN layer as the n-type contact electrode, which was annealed at 850°C for 1 min in N_2 atmosphere to obtain alloy, and a Ni/Au stack was used as the p-type contact electrode, which was annealed at 600°C for 5 min. To characterize the electrical performance for these two DUV-LED chips, both the C–V and I–V characteristics of these two samples are measured by using the Keithley 4200-SCS Semiconductor Device Parameter Analyzer. For the characterization of optical performance, the integrated PL spectra are excited with a 266 nm fourth harmonic YAG:Nd laser as the exciting source, and the temperature-dependent PL light emissions of these two samples are measured at vacuum ambient.

3. Results

To characterize the electrical performance, the EL measurements are carried out at room temperature, and the spectra are presented in Fig. 3. We observe that the EL intensity of sample B is stronger than that of sample A, in detail, the peak intensities of samples A and B are about 4300 and 5586, respectively. As the intensity increase value is in the range of 30%, which is good, then the results mean a significant increase of emisson intensity is obtained in our study. It is also found that the dominant emission peak wavelengths of these two samples are trivial, the values of samples A and B are about 279 nm and 277 nm. Moreover, the electrical performance may be enhanced by inserting the MD growth method of n-AlGaN layer, due to the existence of the MD effect in literatures,[13,17] which may reveal that it could reduce the stress, suppress the dislocations, and decrease the series resistance. Meanwhile, for these two different doping methods in the n-AlGaN layer, the improvements in terms of structure properties have been proven for these two

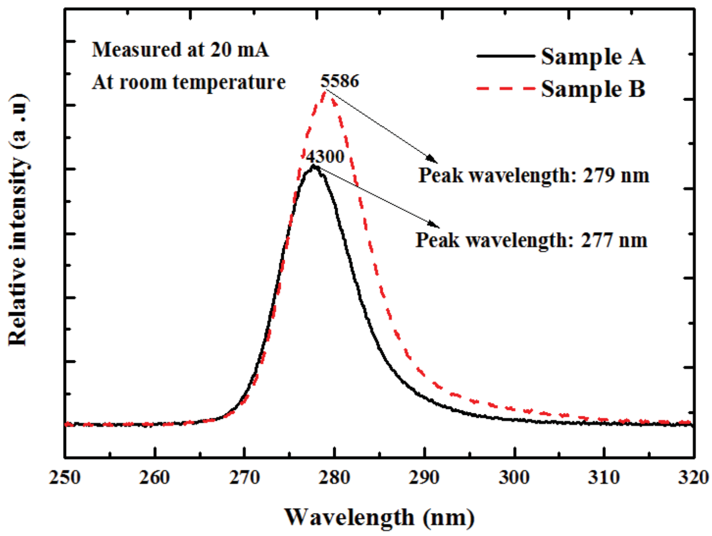

Fig. 3. Measured EL emission spectra of these two samples with different Si-doping growth methods at the driving current of 20 mA.

samples, we note that the main difference between samples A and B is marked with a bidirectional arrow in Fig. 1, which also corresponds to the detailed growth graphs in Fig. 2, we even infer that the doping profile may be broadened by the dopant diffusion processes. These improvements listed above directly correspond to a better current spreading in the epi-layers. Consequently, a homogeneous and high-current-injection efficiency is achieved in sample B, leading to a better electrical performance.

For a further electrical characterization, the I–V characteristics of these two fabricated samples are also measured, as plotted in Fig. 4. Based on the previous researches of our team,[18] through the adoption of these two different growth methods in n-AlGaN layer, we find that the carrier density of samples A and B is about 1.6×10^{18} cm^{-3} and 1.7×10^{18} cm^{-3}. For the measurements of electrical properties of the n-type contacts, the contact resistivity is also a key factor to effectively determine some differences between samples A and B, and the measured sheet resistances is about 390 ($\Omega/\square$) and 360 ($\Omega/\square$), respectively. Besides, we observe that the forward turn-on voltage and reverse current of sample B are smaller than those of sample A. At the typical injected current of 20 mA, the emission spectra of DUV-LEDs are near 280 nm, which directly corresponds to an emission energy near 4.4 eV. The forward voltage of sample B is 7.5 V, whereas a higher value of 9.25 V is observed in sample A, which may be attributed to a worse n-type contact resistance. Once the external reverse bias voltage of 6.2 V is appiled to sample B, the corresponding reverse leakage current is near 0.09 μA, which is about one order of magnitude lower than that of sample A (i.e. 0.8 μA). Meanwhile, seen from the red dash graph in Fig. 4, there is still current flowing below 4.4 V

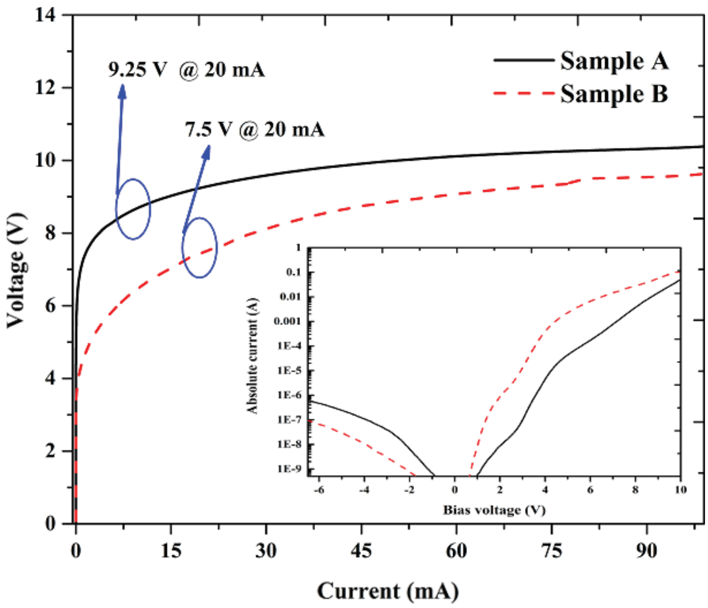

Fig. 4. Measured forward and reverse current versus bias voltage (I–V) characteristics of these two samples at room temperature. The bias voltage for sample B is about 7.5 V, which is near 1.75 V lower than that of sample A (i.e. 9.25 V) at the driving current of 20 mA.

through sample B, it exhibits a small increased leakage current (forward), and it may indicate the problems with the effective current injections.

With respect to the effect of SiH_4 flow rate, and the only difference between these two samples is the growth method of n-AlGaN layer. Considerable stress, which is caused by the lattice dismatch and thermal mismatch, may be effectively relieved. Sample B has better electrical performance by replacing the traditional manufacture process of Si-doping n-AlGaN layer, which is also grown directly on top of the AlN template. Based on the literatures of our team,[19,20] the qualities of AlN template and sapphire substrate between these two samples are always same, there is also an existence of SL buffer layer. Then, the minor improvements may be partly attributed to the possible crystalline quality with decreasing dislocation density in the epi-layers succeeding the investigated MD growth method. In terms of the reverse I–V characteristics, it may be originated from the decreased defect-related components in the processes of the non-radiative recombinations,[21] and even can be operated at low current levels or reverse bias voltages, i.e. without a strong self-heating. Meanwhile, we think that dc stress can induce an increase in the reverse bias current components in sample A. According to the existing literatures for the investigation of propagation of defects in nitrides,[22–24] the results may partly imply that the stress can induce the propagation of defects in the active regions, and there may be a more serious degradation in sample A than those of sample B with modulation SiH_4 flow rate.

Compared with the distinct discrepancy between these two samples with different Si-doping growth methods, and referred to the previous study of our group,[18] the surface morphology values of the epi-layers were measured, and the calculated FWHM is near 10 nm for both samples. In detail, the values of samples A and B are about 7 nm and 12 nm, respectively. Besides, for the peak evalution of the spectral FWHM, we applied the measurement method of the standard deviation between the FWHM and Gaussian peak function, we find that the measured FWHM values of (102) peak in samples A and B are about 349 arcsec and 277 arcsec, respectively. Estimated from the atomic force microscope measurements with a lateral size of 2 μm, the measured roughness of surface is about 1.6 nm and 1.3 nm, the results mean that these two different doping methods almost have little impact on the surface.

It has been claimed that the enhanced internal capacitance of P–N junction could strengthen the electrical performance,[25] which depends on the variation of the applied bias voltages. Also, it was reported that the internal capacitance could be controlled by the different Si-doping levels.[26] To investigate the improved electrical performance, both set-ups adopt the commonly used equivalent circuit model, which is composed of a capacitor and a conductor connected in parallel.[27] Moreover, the circuit models utilized in extracting the internal capacitance of P–N junction diode are exhibited, as shown in Figs. 5(a) and 5(b). The variation of the internal capacitance of P–N junction is a relatively complicated process in our study, and in the case of ensuring the same influence of the external experimental environment for the measurements, such as, setup, probes, contact pressure, etc. Besides, the applied C–V measurement has a better accuracy than the high-frequency probe test, thus, we can think that it even can reduce the errors caused by cabling or

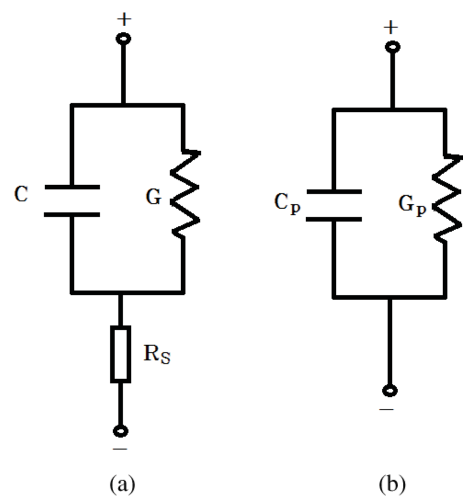

Fig. 5. The circuit models of P–N junction in UV-LEDs utilized in extracting the internal capacitance for these two samples. (a) The equivalent circuit and (b) the measured circuit.

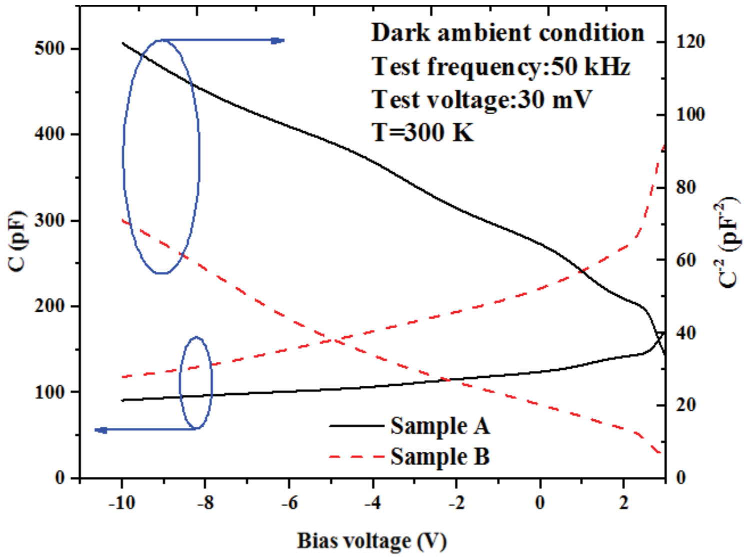

Fig. 6. Measured internal capacitance versus voltage (C–V) and C^{-2} versus V (C^{-2}–V) characteristic curves of these two samples as a function of reverse bias voltage.

device series resistance for UV-LEDs.[28] Before the package of DUV-LED chips, the convenient methods of C–V measurements were carried out at the test conditions of 30 mV and 50 kHz.

To further investigate the relationships between the internal capacitance and the electrical properties, both the measured C–V datas and C^{-2} versus V plots are shown in Fig. 6. According to the previous researches,[29] the P–N junction diode also can be regarded as a simplified circuit model of the parallel plate capacitor, in our case, the capacitance can be expressed as follows:

$$\mathrm{C} = A\frac{\varepsilon_s}{W_d}\,, \tag{1}$$

where A is the area of the parallel plate, ε_s is the dielectric constant of the components, W_d is the width of the depletion layer in the active regions.

Then, the C–V characteristics for the P–N junction diode can be expressed as the following formulas, knowing that[30]:

$$\mathrm{C} = \sqrt{\frac{q\varepsilon_s NA^2}{2(V_{bi}+V_r)}} = \sqrt{\frac{q\varepsilon_0\varepsilon_r NA^2}{2(V_{bi}+V_r)}}\,, \tag{2}$$

$$\frac{1}{C^2} = \frac{2(V_{bi}+V_r)}{q\varepsilon_0\varepsilon_r NA^2}\,, \tag{3}$$

where ε_r is denoted as the relative dielectric constant, ε_0 is the vacuum permittivity constant, q is the unit charge, N is the apparent carrier concentration, which is closely related to W_d, and V_{bi} is the built-in potential barrier voltage, which is regarded as the critical value.

Seen from the graphs in Fig. 6, as a whole, there is an obvious difference between these two samples, i.e. the internal capacitance of sample B is much larger than that of sample A. In detail, the C–V curves of sample B comparatively have a fast rate of change. Especially, the peak intensity of internal capacitance is obtained earlier in sample B, corresponding to a smaller turn-on voltage, it also shows a faster drop rate afterwards. The measured peak capacitance of the MD sample is up to 370 pF, whereas that for one of the UD samples is only 180 pF. Moreover, derived from the C–V datas at 50 kHz, the C^{-2}–V curves at the reverse bias are also plotted above. It is found that the slopes of C^{-2}–V curves in these two samples are similar, which is consistent with the conclusion of Refs. 9 and 31. Since the only difference of these two samples is determined by the n-AlGaN layer, and all the rest of the growth processes are kept the same in our experiments, then it is also proved that there is no difference in the growth of the p-type layer. The reduced reverse leakage current of sample B is attributed to the decreased rate of related current leakage paths with the capacitance modulation effect other than the factors mentioned above, such as the better AlN template or the less defective substrate.

Based on the previous literatures,[32–34] we even infer that the Si-MD growth methods may lead to the formation of the periodically modulated doping SL regions, which can behave like a series of capacitors in our experiments, and these capacitors can effectively enhance the peak internal capacitance. Compared with these two doping methods in our structures, and combined with the related physical mechanisms for the analysis, it also can be understood from the point of the built-in electric field effect.[35] Furthermore, we also think that these capacitors can be caused by the built-in electric fields inside the AlGaN epi-layers along the growth direction (0001) sapphire substrate, and the built-in electric fields can lead to an increase in the charge accumulations at the interfaces of every modulated doping region. Referring to the previous results of the related works,[11,25] and considering the built-in electric field effect, we can even probably conclude that the corresponding SLs of n-AlGaN layers should not be square well, instead, it should be tilted wells, which also may be attributed to the MD growth procedures,[14,18] as shown in Fig. 2(b).

To effectively characterize the effect of built-in electric field characteristics for these two samples, the related optical performance of the PL spectra with these two different Si-doping methods in every n-AlGaN layer is further investigated, respectively. As shown in Fig. 7, both these two samples are measured at a low temperature of about 10 K due to the fact that PL intensity decreases with the increasing ambient temperature, and the PL characteristics are slowly quenched with the increasing temperature. Seen from the relative intensity plotted in the graphs, it is clear to find that the PL intensity is much higher in sample B than that of sample A. Moreover, the results are consistent with our conjectures we just put forward above.

Moreover, referring to the existing literatures,[32,35,36] we further have conducted an estimation for the inensity values of built-in electric fields inside these

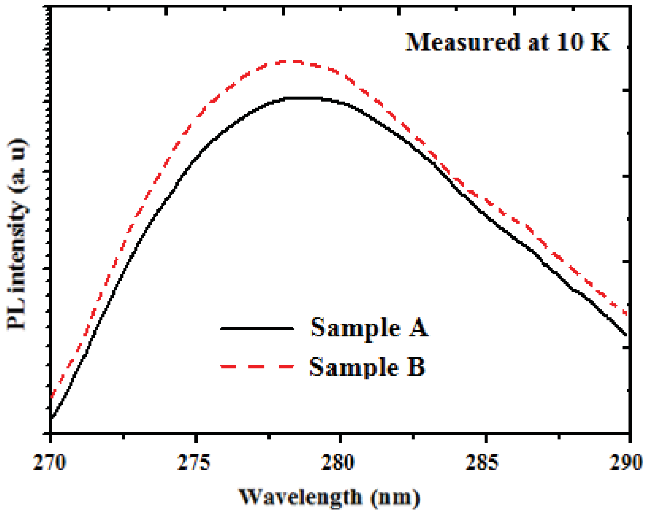

Fig. 7. Measured PL spectra characteristics for these two structures at a low testing temperature.

two samples. In detail, as for the barriers are finite in this case, and it is of 40-period monolayer's strucures, and it is about 25 nm thickness for every monolayer. Also, the SLs corresponding to the wells are kept the same with another 40-period thickness in sample B. For the III–V nitride devices, it is the total polarization difference between the well and barrier regions that could produce the built-in electric fields within these two materials. In our work, for the SL structures, there is a difference in total polarization intensity between these two polarizations, which is denoted as ΔP, and it can be given by[32]

$$\Delta P = P_b - P_w \,, \tag{4}$$

where P_b represents the total polarization intensity within the barrier material, and P_w is the total polarization intensity in the well material. Thus, the electric fields, which are produced within the well regions and the barrier regions can be further written as[35,37]:

$$E_w = \frac{l_b \Delta P}{l_w \varepsilon_b \varepsilon_0 + l_b \varepsilon_w \varepsilon_0} = \frac{l_b (P_b - P_w)}{\varepsilon_0 (l_w \varepsilon_b + l_b \varepsilon_w)} \,, \tag{5}$$

$$E_b = \frac{l_w (P_b - P_w)}{\varepsilon_0 (l_w \varepsilon_b + l_b \varepsilon_w)} \,. \tag{6}$$

Here, ε_w is denoted as the dielectric constant of the well layers, and ε_b represents the dielectric constant of the barrier layers, which can be attributed to the different values of ε for these two wells and barriers. l_b is the barriers thickness, l_w corresponds to the wells thickness. By using these formulas listed above and the calaulated values of spontaneous polarization, the internal electric field strength of about 1250 kV/cm is roughly deduced in sample B, which is much larger than that of 1000 kV/cm in sample A. Namely, it reveals that the sample B with Si-MD methods is of a stronger built-in electric field intensity. On the other hand, in our experiments, the results are also in good agreement with the PL characteristics measured above.

Based on previous researches, LEDs with enhanced internal capacitance were more resistant to external ESD impulses, the problems for devices' reliability have been reported, and the effect of capacitance modulation was studied.[38–40] Once the increasing reverse bias voltage (V_r) is applied to LED, an improved mechanism can be discovered in sample B as responsible for the increased capacitance due to the generation of non-radiative centers. Moreover, it also can be triggered by the flow of current, and correlated to the decreased defectiveness in the active regions, with a subsequent decrease in the non-radiative recombination rate. Owing to the minor crystalline quality improvements in sample B, possible explanations about the influence of inserting the MD n-AlGaN layer on the material quality of the subsequent epi-layers may be proposed to better understand the relationships between the electrical performance and the internal capacitance with the MD growth techniques.[41]

Considering the existence of capacitance modulation effect and decreased series resistance in sample B, W_d decreases more quickly with the decrease of reverse bias voltage. It means less screw dislocations, which result in the reduced related current leakage paths. The result is also consistent with the conclusion of the measured I–V characteristics, as shown in Fig. 4. At this time, the n-type vacancy of the donor defects decreases, whereas the concentration of the Mg hole is high, and it restricts the increase of the donor concentrations. These above listed behaviors may lead to improvements on the active regions, which is induced by the direct current stress, due to the decrease of non-radiative recombination centers with the capacitance modulation effect. In this case, the internal capacitance reduces more greatly, and it presents a more pronounced downward trend in sample B than in sample A. Even for higher reverse bias levels, the active regions are fully depleted more quickly in sample B. Moreover, the space charge region will penetrate into the n-type region more easily. Correspondingly, the reverse I–V characteristics also show an earlier saturated state with a lower reverse leakage current.

In fact, sample B has a higher internal capacitance than that of sample A, which also corresponds to the measured I–V characteristics.[42] Thus, we can think that there is a lower series resistance by inserting the Si-MD n-AlGaN layer. As for the improved current spreading properties, the possible minor improvements on the material quality may lead to a better electrical performance with the MD growth method due to the capacitance modulation effect. These above listed explanations can be ascribed as the reasons for the enlarged internal capacitance. There is a difference by inserting the Si-MD n-AlGaN layers in DUV-LEDs, which also may be accounted for the presence of the interface states. Subsequently, the doping concentration is different between the quantum well layers and the barrier layers, leading to a direct change of the interface state charge densities in the active regions. As for the MD growth techniques incorporated in n-AlGaN layers, the Si dopants in MD layer may be confined at certain locations ideally as we previously designed. The crystalline quality improvements reduce the carrier scatter centers as a reduction in dislocation. Meanwhile, we observed that the doping profile may be broadened by the dopant diffusion processes, and a better doping profile and minor material quality improvements were achieved in sample B. By means of C–V profiling, once a varied current stress is formed, the distribution of the space charge in the active regions can significantly be changed with the Si-MD n-AlGaN layers. Seen from the results of measured C–V characterization, it presents an effective way for the analysis on the distribution of the charged carriers and the apparent charge distribution of free carriers in the P–N junction diodes, which can arise from a consequence of the stress.

4. Conclusions

In summary, the commonly Si-UD growth methods of n-AlGaN layer and the Si-MD n-AlGaN layer for DUV-LEDs, respectively, have been grown. The influence of these two Si-doping methods in AlGaN layers on the electrical characteristics has been investigated, and the internal capacitance characteristics are discussed based on the enhanced I–V characteristics and light emission measurements. Moreover, due to the existence of the periodic MD regions in n-AlGaN SLs layers, which can behave like a series of capacitors, both the measured capacitance–voltage characteristics and the PL intensity with the Si-MD growth method are effectively enhanced. In detail, the effects of these capacitors can enhance the peak internal capacitance up to 370 pF in the MD samples, whereas the Si-UD sample is only 180 pF. We thus demonstrate that the enhanced electrical performance is attributed to the internal capacitance modulation effect, meanwhile, the enhanced performace of LEDs may be partly influenced by the minor crystalline quality improvements in the epi-layers succeeding the Si-MD n-AlGaN layer. The presented results provide potential applications to the research of electrical performance for DUV-LEDs with the MD growth method. We hope this investigation of the Si-MD growth methods will be usefull for developing some DUV-LEDs with better performance.

Acknowledgments

This work was supported by the National Natural Science Foundation of China for Excellent Young Scholars (No. 61622404), National Natural Science Foundation of China (No. 61177052), National Key Research & Development Program of China (No. 2016YFB0400803), the National Natural Sciences Foundation of China (No. 61527814), Beijing Nova Program Z181100006218007, the Science & Technology Planning Projects of Guangdong Province, China under Grant No. 2015B010114007.

References

1. M. A. Khan, M. Shatalov, H. P. Maruska, H. M. Wang and E. Kuokstis, *Jpn. J. Appl. Phys.* **44** (2005) 7191.
2. A. Khan, B. K and K. T, *Nat. Photonics* **2** (2008) 77.
3. E. F. Schubert and J. K. Kim, *Science* **308** (2005) 1274.
4. J. Cho, E. F. Schubert, J. K. Son, D. Y. Kim and J. K. Kim, *Electron. Mater. Lett.* **10** (2014) 1155.
5. W. Liu *et al.*, *J. Alloys Compd.* **725** (2017) 1130.
6. C. Pietzka, G. Li, M. Alomari, H. Xing, D. Jena and E. Kohn, *J. Appl. Phys.* **112** (2012) 074508.
7. H. P. Nguyen *et al.*, *Nano Lett.* **11** (2011) 1919.
8. C. Bilkan, A. Gumus and S. Altmdal, *Mater. Sci. Semicond. Process.* **39** (2015) 484.
9. D. P. Han, Y. J. Kim, J. I. Shim and D. S. Shin, *IEEE Photonics Technol. Lett.* **28** (2016) 2407.
10. M. Meneghini, A. Tazzoli, G. Mura, G. Meneghesso and E. Zanoni, *IEEE T. Electron Dev.* **57** (2010) 108.
11. Y. B. Pan *et al.*, *J. Cryst. Growth* **286** (2006) 255.
12. G. Y. Zhao, M. Adachi, H. Ishikawa, T. Egawa, M. Umeno and T. Jimbo, *Appl. Phys. Lett.* **77** (2000) 2195.
13. Z. Y. Zheng *et al.*, *Appl. Phys. Lett.* **99** (2011) 111109.
14. T. C. Wen *et al.*, Improved ESD reliability by using a modulation doped $Al_{0.12}Ga_{0.88}NGaN$ superlattice in nitride-based LED, *2003 International Semiconductor Device Research Symp.*, December 2003.
15. P. P. Li *et al.*, *IEEE Photonic. Technol. Lett.* **27** (2015) 2004.
16. H. M. Kim, T. W. Kang and K. S. Chung, *Adv. Mater.* **15** (2003) 567.
17. T. C. Wen, S. J. Chang, C. T. Lee, W. C. Lai and J. K. Sheu, *IEEE T. Electron Dev.* **51** (2004) 1743.
18. Z. Shaoxin, Y. Jianchang, Z. Jianping, Z. Ning and S. Zhao, *J. Semicond.* **34** (2013) 053004.
19. J. Yan, Y. Tian, X. Chen, Y. Zhang, J. Wang and J. Li, *Phys. Status Solidi C* **13** (2016) 228.
20. J. Yan, J. Wang, Y. Zhang, P. Cong, L. Sun, Y. Tian *et al.*, *J. Cryst. Growth* **414** (2015) 254.
21. T. H. Chiang *et al.*, *IEEE Photonics Technol. Lett.* **24** (2012) 800.
22. L. Kevin, G. Thomas, T. Darren, C. Eric, R. Pradeep, S. Tim, B. Dale and D. Robert, *Appl. Phys. Lett.* **75** (1999) 196.
23. K. Asif, B. Krishnan and K. Tom, *Nat. Photonics* **2** (2008) 77.
24. T. N. Oder, K. H. Kim, J. Y. Lin and H. X. Jiang, *Appl. Phys. Lett.* **84** (2004) 466.
25. M. K. Kwon, K. Park, S. H. Baek, J. Y. Kim and S. J. Park, *J. Appl. Phys.* **97** (2005) 48.
26. S. K. Jeon *et al.*, *Appl. Phys. Lett.* **94** (2009) 131106.
27. D. K. Schroderauth, *Semiconductor Material and Device Characterization* (John Wiley & Sons, 2006).
28. Z. Lv, Y. Xu and Y. Ruan, The capacitance measurement of LED, *China Light & Lighting* (2010).
29. L. Wang *et al.*, *Jpn. J. Appl. Phys.* **47** (2008) 7101.
30. S. M. Sze and K. K. Ng, *Physics of Semiconductor Devices* (John Wiley & Sons, New Jersey, 2007).
31. B. Kinaci and S. Ozcelik, *J. Electron. Mater.* **42** (2013) 1108.
32. S.-P. Wan, J.-B. Xia and K. Chang, *J. Appl. Phys.* **90** (2001) 6210.

33. M. S. Miao, Q. Yan, C. G. Van de Walle, W. K. Lou, L. L. Li and K. Chang, *Phys. Rev. Lett.* **109** (2012) 186803.
34. D. Zhang, W. Lou, M. Miao, S.-C. Zhang and K. Chang, *Phys. Rev. Lett.* **111** (2013) 156402.
35. M. Leroux, N. Grandjean, M. Laugt and J. Massies, *Phys. Rev. B* **58** (1998) R13371(R).
36. S.-H. Wei and A. Zunger, *Appl. Phys. Lett.* **72** (1998) 2011.
37. F. Bernardini and V. Fiorentini, *Phys. Rev. B* **64** (2001) 085207.
38. C. X. Wang *et al.*, *Jpn. J. Appl. Phys.* **52** (2013) 102103.
39. S. C. Yang *et al.*, *Jpn. J. Appl. Phys.* **49** (2010) 056602.
40. S. C. Yang *et al.*, *Microelectron. Reliab.* **50** (2010) 959.
41. C. C. Hu, *Modern Semiconductor Devices for Integrated Circuits* (Pearson, 2009).
42. Z. Shi *et al.*, *Appl. Phys. Express* **7** (2014) 082102.